Atmospheric Correction Algorithms for Remote Sensing of Land and Water Surfaces

Bo-Cai Gao[1]

[1]Remote Sensing Division,
Naval Research Laboratory, Washington, DC USA

OUTLINE

- Atmospheric corrections over land
- Atmospheric corrections over water
- Discussions and summary

Atmospheric Correction Over Land

An AVIRIS Spectrum

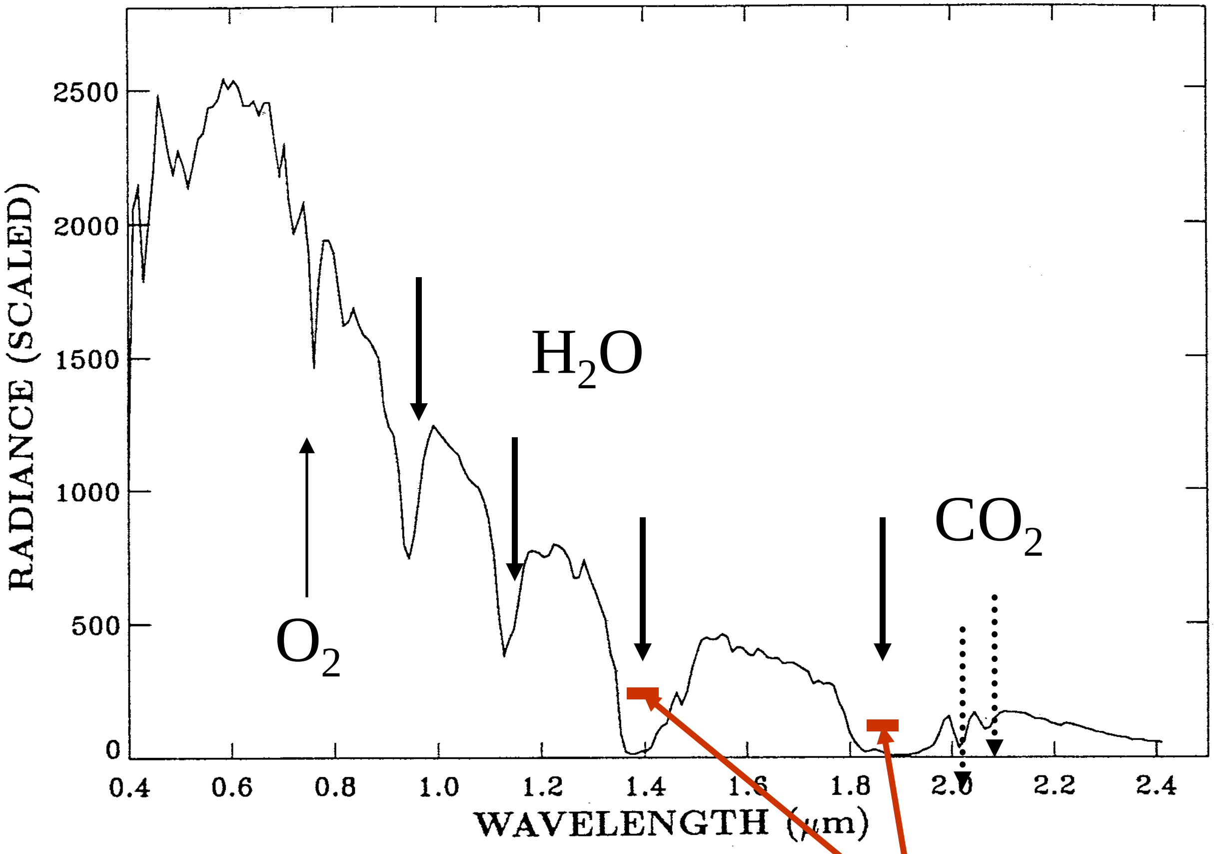

The AVIRIS spectrum is affected by atmospheric absorption and scattering effects. In order to obtain the surface reflectance spectrum, the atmospheric effects need to be removed.

Strong water vapor bands are located near 1.38 and 1.88 micron. No signals are detected under clear sky conditions.

Aerosol Scattering Effects

True Color Image (R: 0.66, G: 0.55, B: 0.47 μm) | False Color Image (R: 2.13, G: 1.24, B: 1.64 μm)

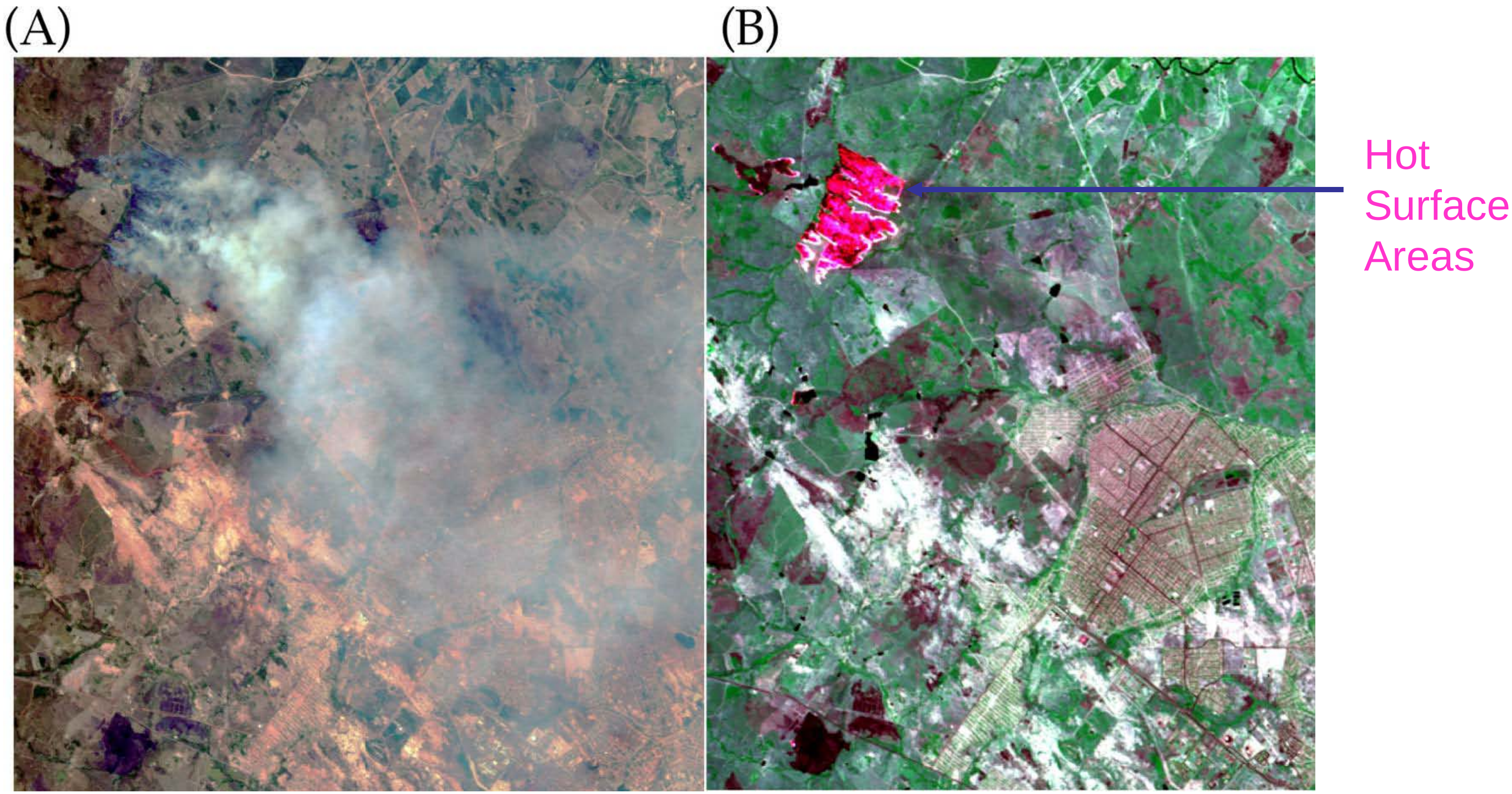

Smoke is seen in visible channel images, but disappears in the near-IR channel images. Smoke particle size is ~0.1 – 0.2 μm.

Equations For Atmospheric Correction Over Land

The measured radiance at the satellite level can be expressed as:

$$L_{obs} = L_a + L_{sun}\, t\, \rho \qquad (1)$$

L_a: path radiance;
ρ : surface reflectance;
L_{sun}: solar radiance above the atmosphere;
t: *2-way transmittance for the Sun-surface-sensor path*

Define the satellite apparent reflectance as

$$\rho^*_{obs} = \pi\, L_{obs} / (\mu_0\, E_0) \qquad (2)$$

$$\rho^*_{obs} = T_g\, [\, \rho_a + t\, \rho / (1 - \rho\, s)\,] \qquad (3)$$

By inverting Eq. (3) for ρ, we get:

$$\rho = (\rho^*_{obs}/T_g - \rho^*_a) / [t + s\, (\rho^*_{obs}/T_g - \rho^*_a)\,] \qquad (4)$$

Gao, B.-C., K. H. Heidebrecht, and A. F. H. Goetz, Derivation of scaled surface reflectances from AVIRIS data, *Remote Sens. Env., 44*, 165-178, 1993.

SAMPLE REFLECTANCE RETRIEVALS OVER MINERAL

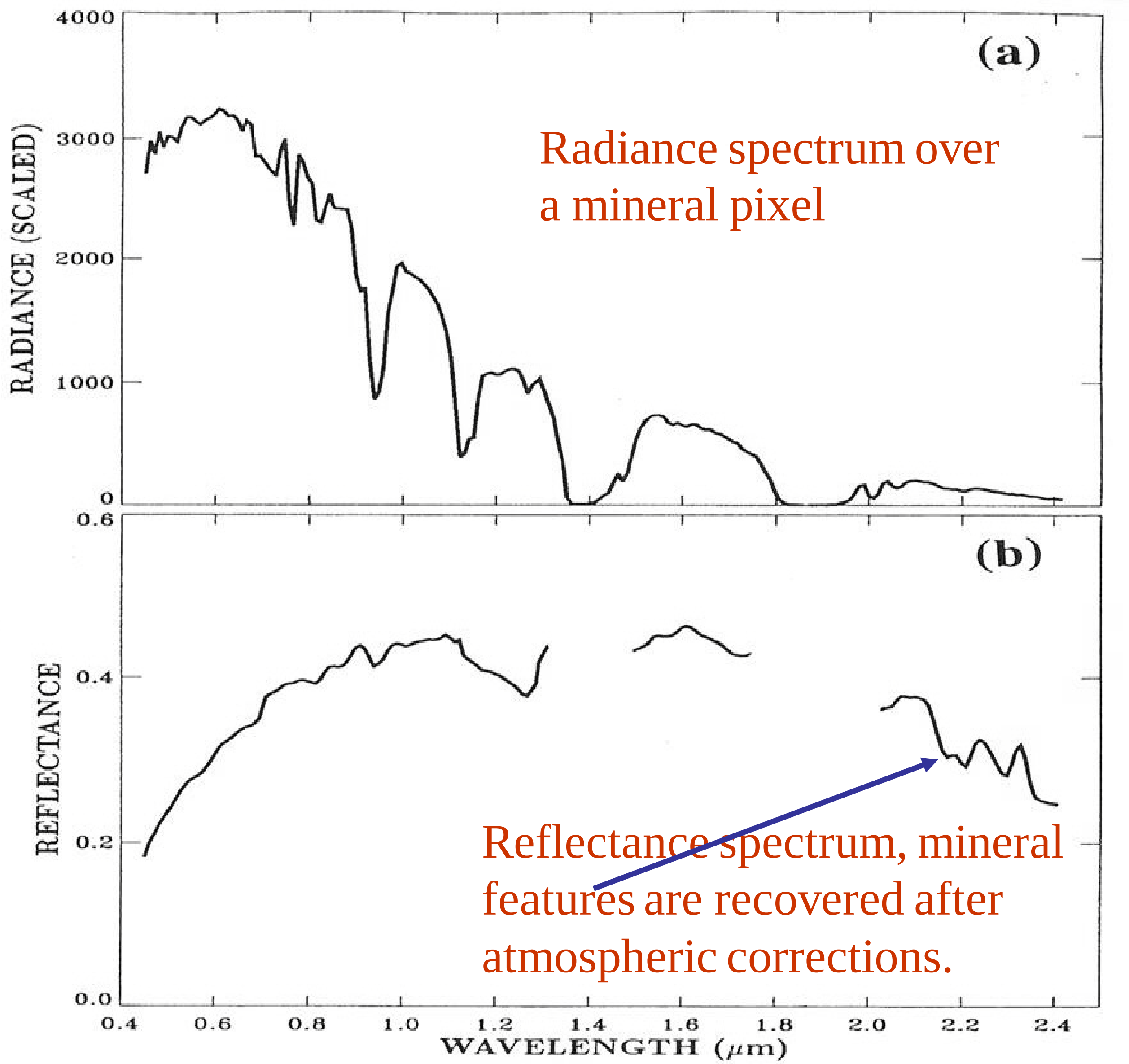

MINERAL MAPPING USING ATREM OUTPUT

by Scientists at USGS in Denver, Colorado

RGB Image (Cuprite, NV)

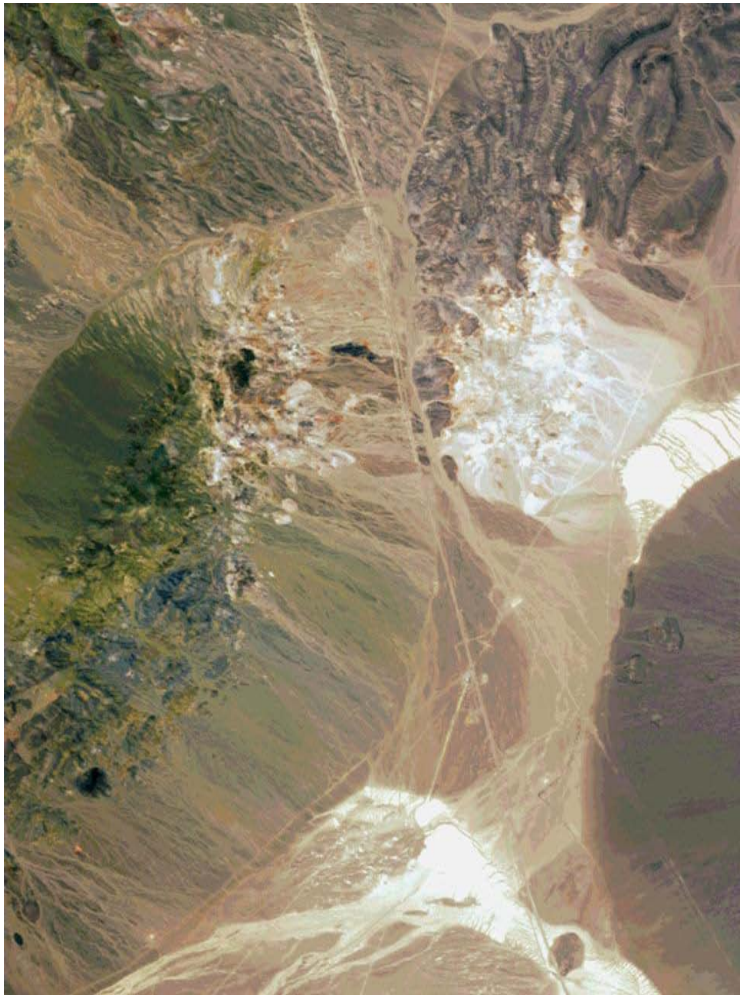

USGS Mineral Map, ~11x18 km

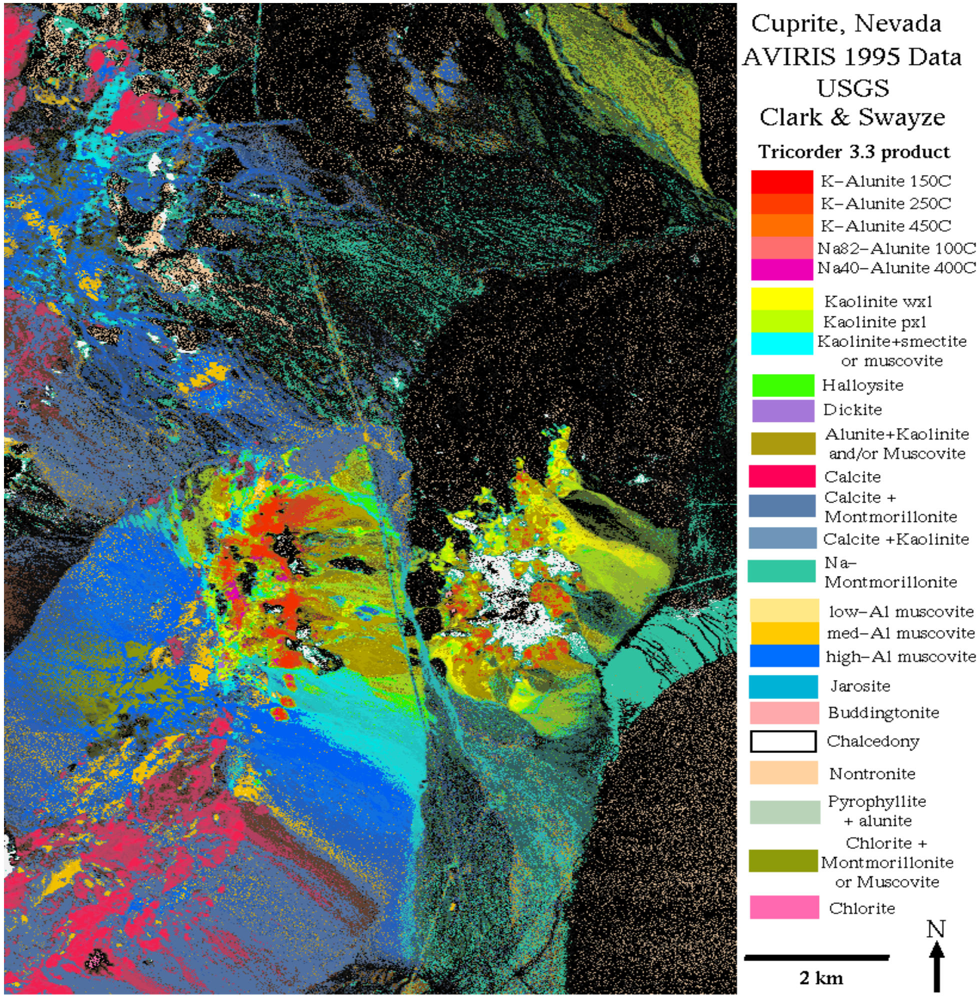

SAMPLE REFLECTANCE RETRIEVALS WITH ATREM

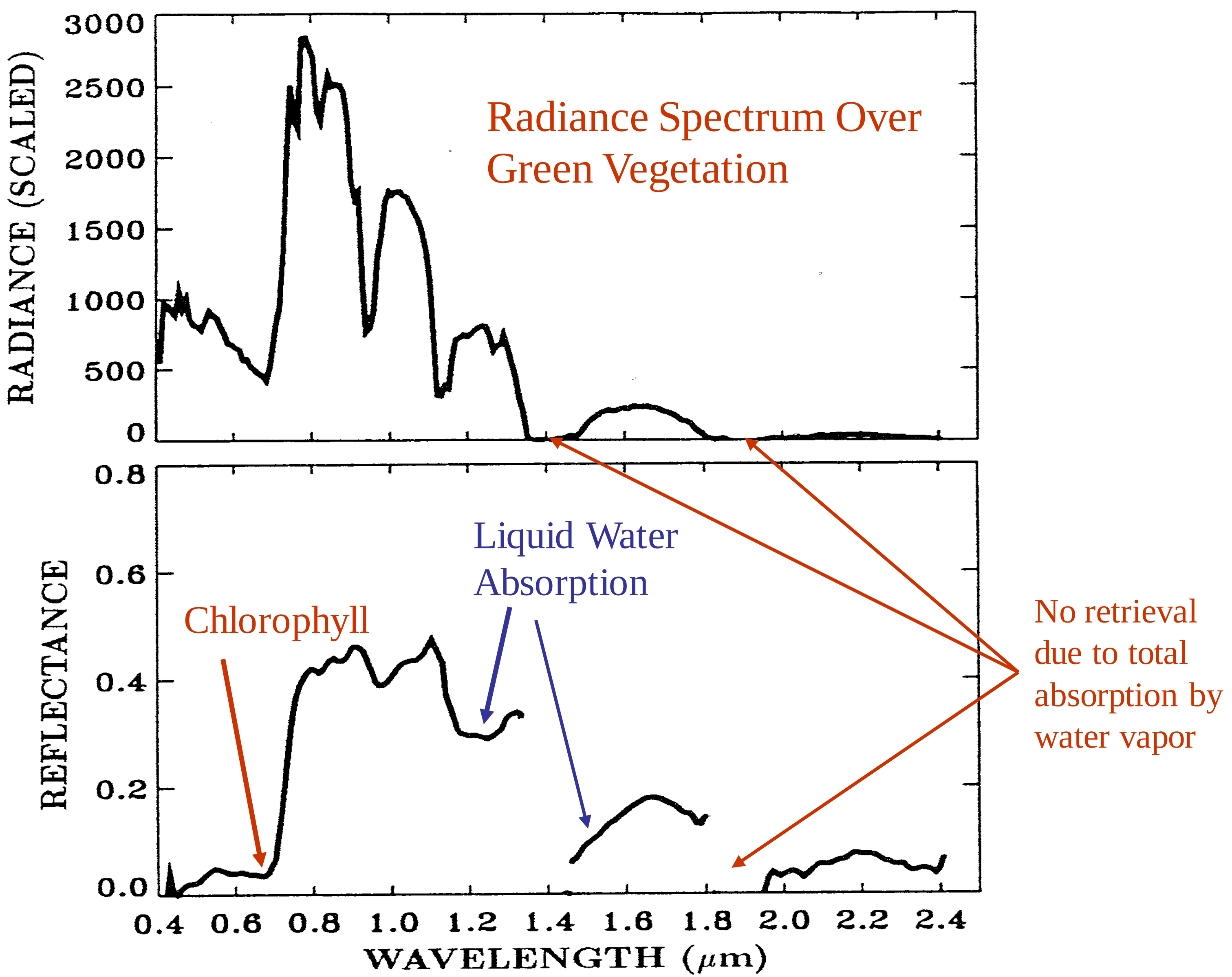

Vegetation Functional Type Analysis, Santa Barbara, CA

Dar Roberts, et al, UCSB

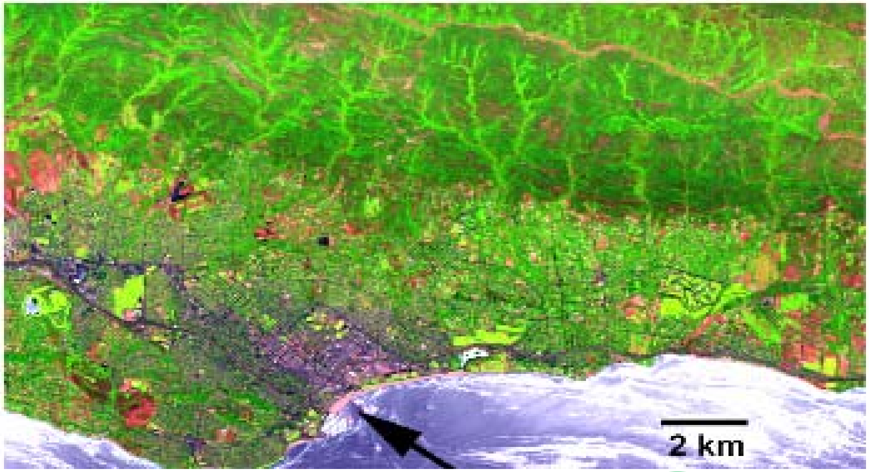

MESMA Species Type 90% accurate

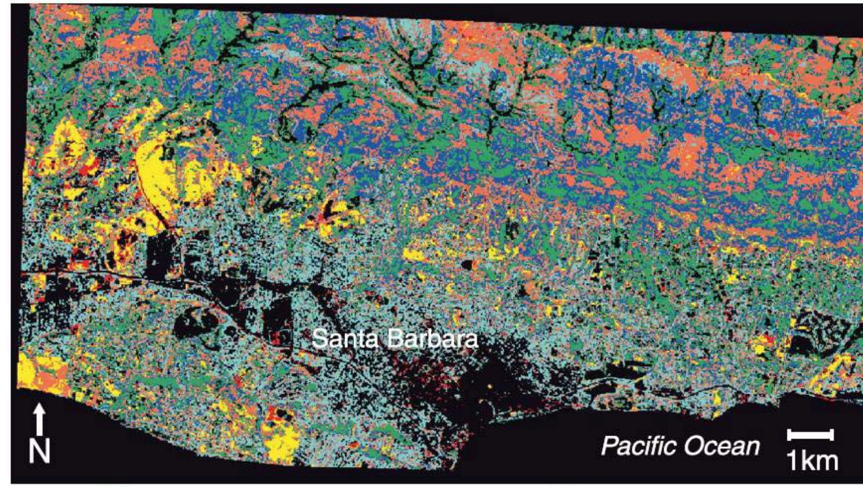

Adenostoma fasciculatum | *Quercus agrifolia*
Ceanothus megacarpus | Grass
Arctostaphylos spp. | Soil

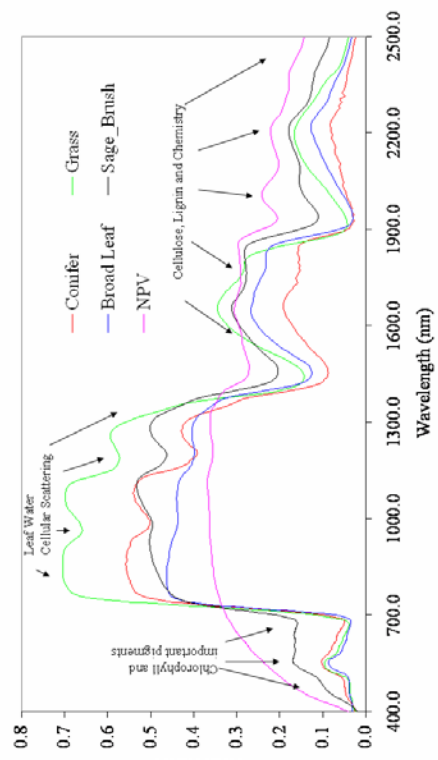

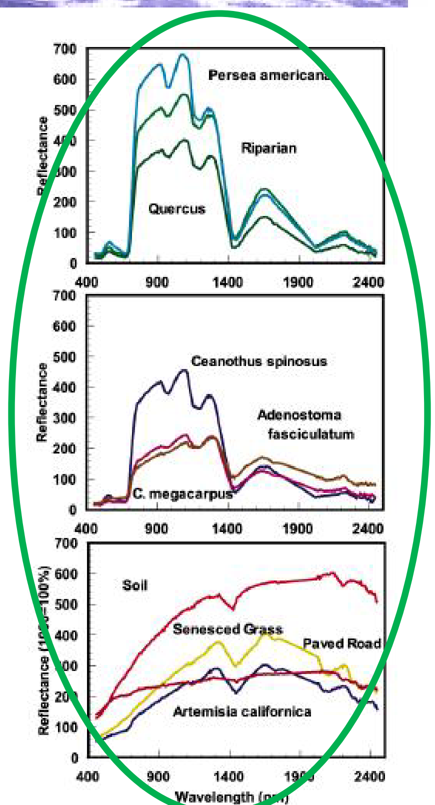

Species Fractional Cover

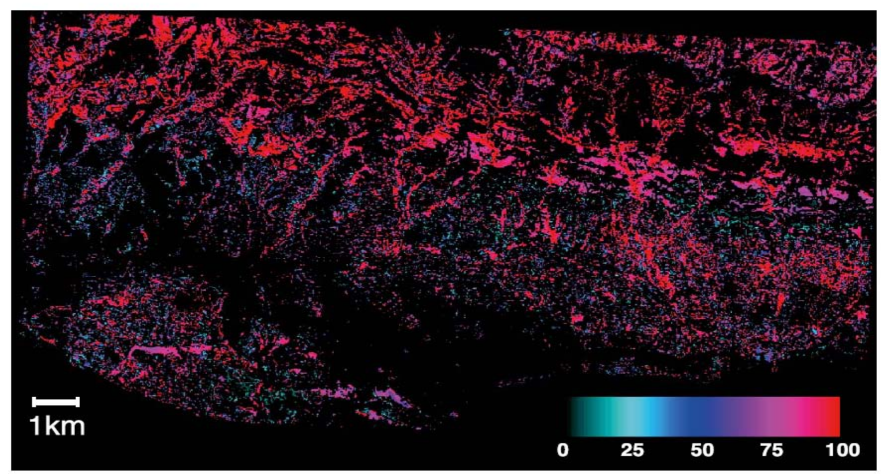

Examples of Cirrus Detection & Corrections

AVIRIS data acquired over Bowie, MD in summer 1997

CIRRUS IMAGE (1.38μm)

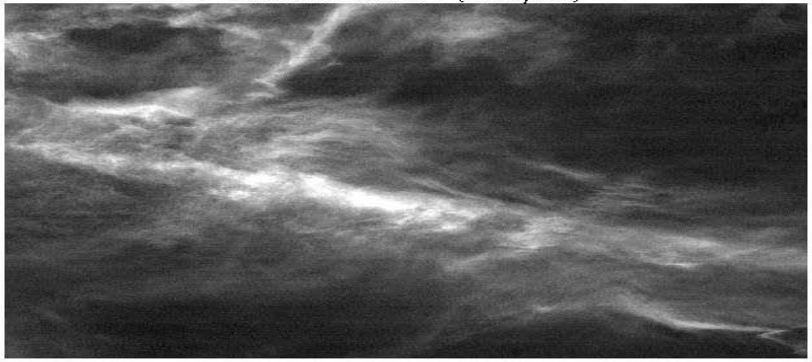

CIRRUS–CORRECTED IMAGE

Atmospheric Correction Over Water

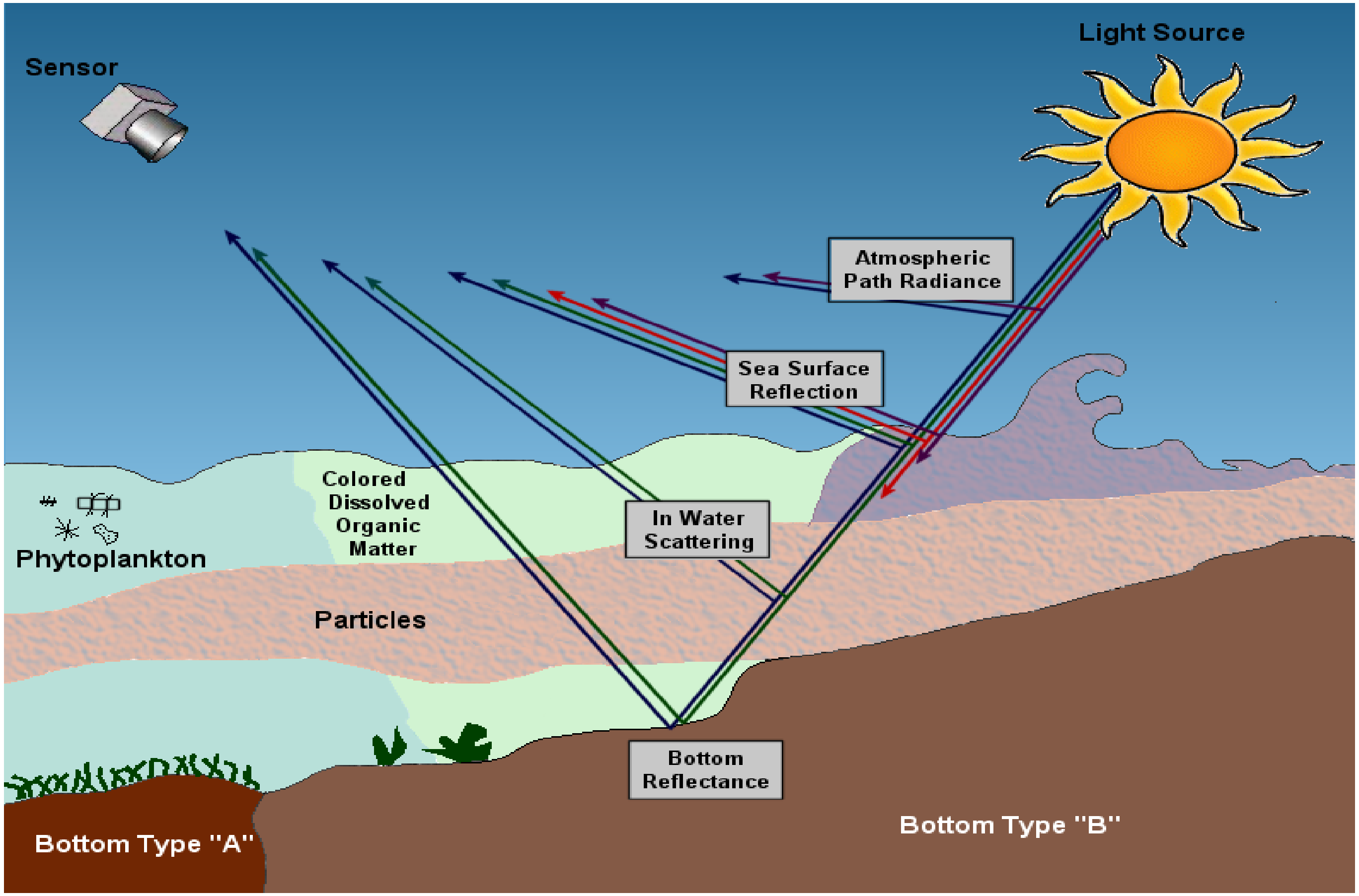

Over the dark water surfaces, ~90% of satellite radiances come from the atmosphere, and ~10% come from water. Very accurate atmospheric corrections are required in order to derive the useful water leaving reflectances. The specular reflection at the air/water interface introduces additional complications for modeling.

An AVIRIS Spectrum Over A Water Pixel

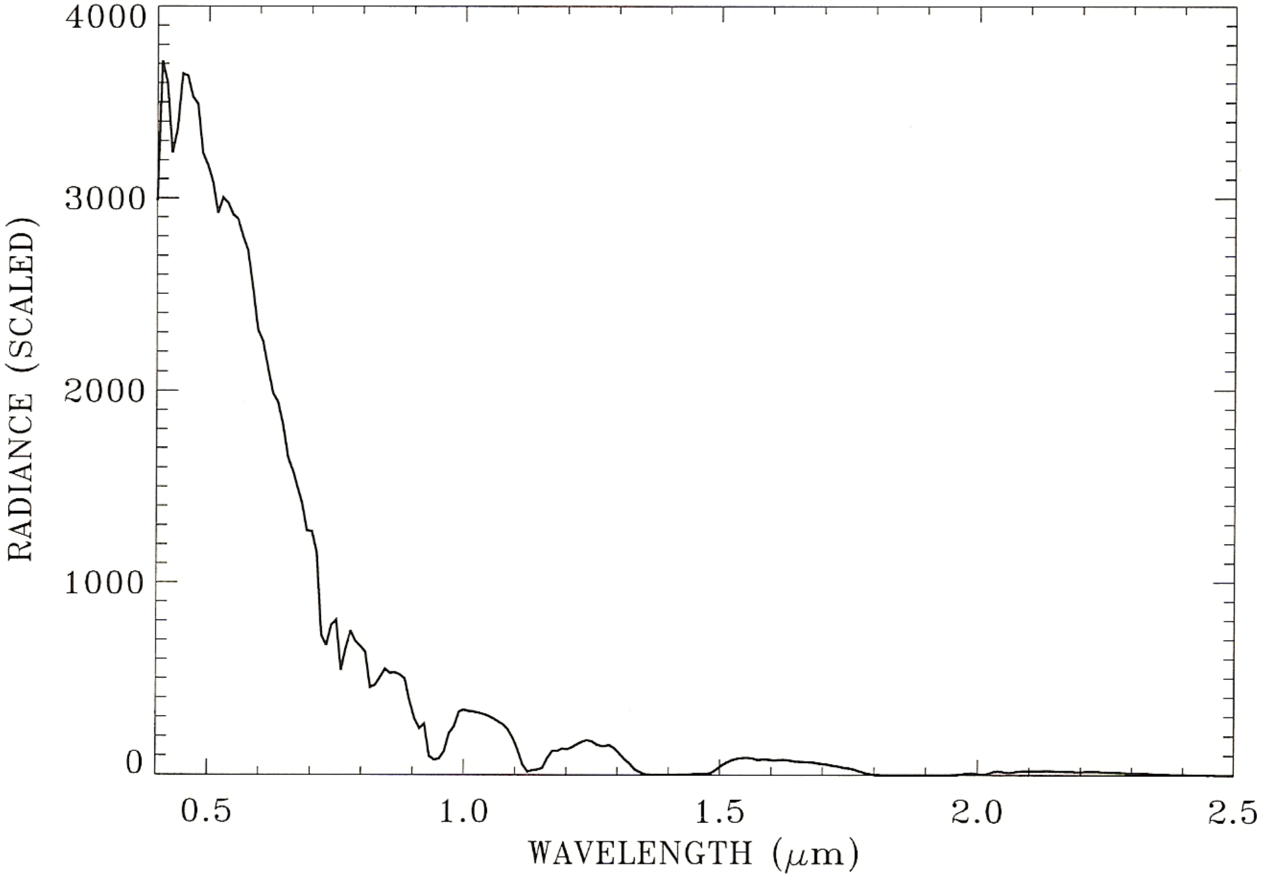

The radiances above one micron are very small.

Relevant Equations and Definitions

In the absence of gas absorption, the radiance at the satellite level is:

$$L_{obs} = L_0 + L_{sfc}\, t'_u + L_w\, t_u, \qquad (1)$$

L_0: path radiance; L_w: water leaving radiance;

L_{sfc}: radiance reflected at water surface; t_u*: upward transmittance*

Define $$L_{atm+sfc} = L_0 + L_{sfc}\, t'_u \qquad (2)$$

Eq. (1) becomes: $$L_{obs} = L_{atm+sfc} + L_w\, t_u \qquad (3)$$

Multiply Eq. (3) by π and divide by ($\mu_0\, E_0$), Eq. (3) becomes:

$$\pi\, L_{obs} / (\mu_0\, E_0) = \pi\, L_{atm+sfc} / (\mu_0\, E_0) + \pi\, L_w\, t_d\, t_u / (\mu_0\, E_0\, t_d\,) \qquad (4)$$

Several reflectances are defined as:

Satellite apparent reflectance: $$\rho^*_{obs} = \pi\, L_{obs} / (\mu_0\, E_0), \qquad (5)$$

$$\rho^*_{atm+sfc} = \pi\, L_{atm+sfc} / (\mu_0\, E_0), \qquad (6)$$

Water leaving reflectance: $$\rho_w = \pi\, L_w / (\mu_0\, E_0\, t_d\,) = \pi\, L_w / E_d \qquad (7)$$

Remote sensing reflectance: $$R_{rs} = \rho_w / \pi = L_w / E_d \qquad (7')$$

Substitute Eqs (5) – (7) into Eq. (4): $$\rho^*_{obs} = \rho^*_{atm+sfc} + \rho_w\, t_d\, t_u \qquad (8)$$

After consideration of gas absorption and multiple reflection between the atmosphere and surface and with further manipulation, we can get:

$$\rho_w = (\rho^*_{obs}/T_g - \rho^*_{atm+sfc}) / [t_d\, t_u + s\, (\rho^*_{obs}/T_g - \rho^*_{atm+sfc})\,] \qquad (11)$$

Gao, B.-C., M. J. Montes, Z. Ahmad, and C. O. Davis, Atmospheric correction algorithm for hyperspectral remote sensing of ocean color from space, Appl. Opt., 39, 887-896, February 2000.

Atmospheric Correction for Water Surfaces

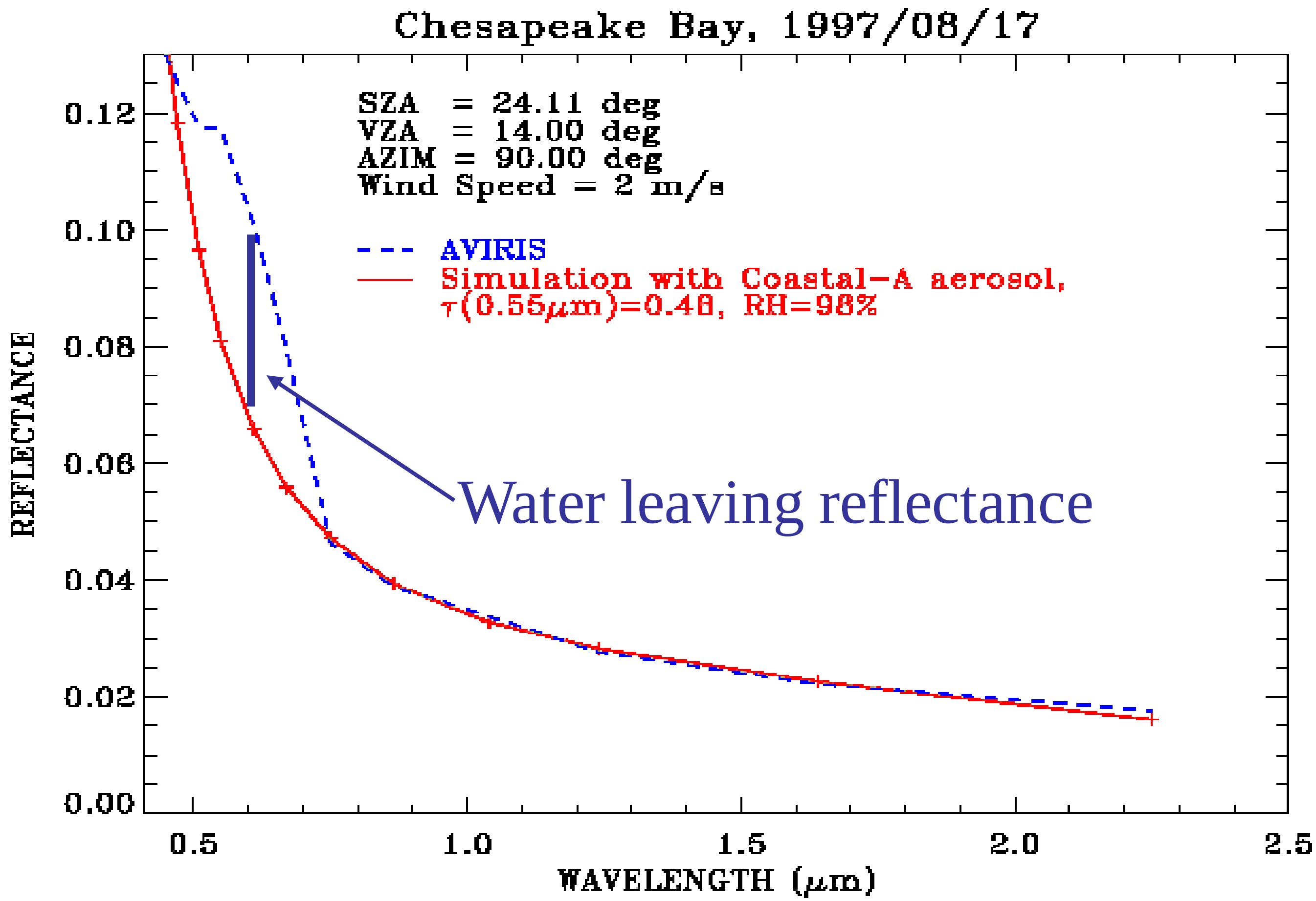

Channels at 0.86 and longer wavelengths are used to estimate atmospheric effects, and then extrapolate to the visible region. The differences between the two curves above are proportional to water leaving reflectances.

An Example of Ocean Atmospheric Correction Including Surface Glint Correction

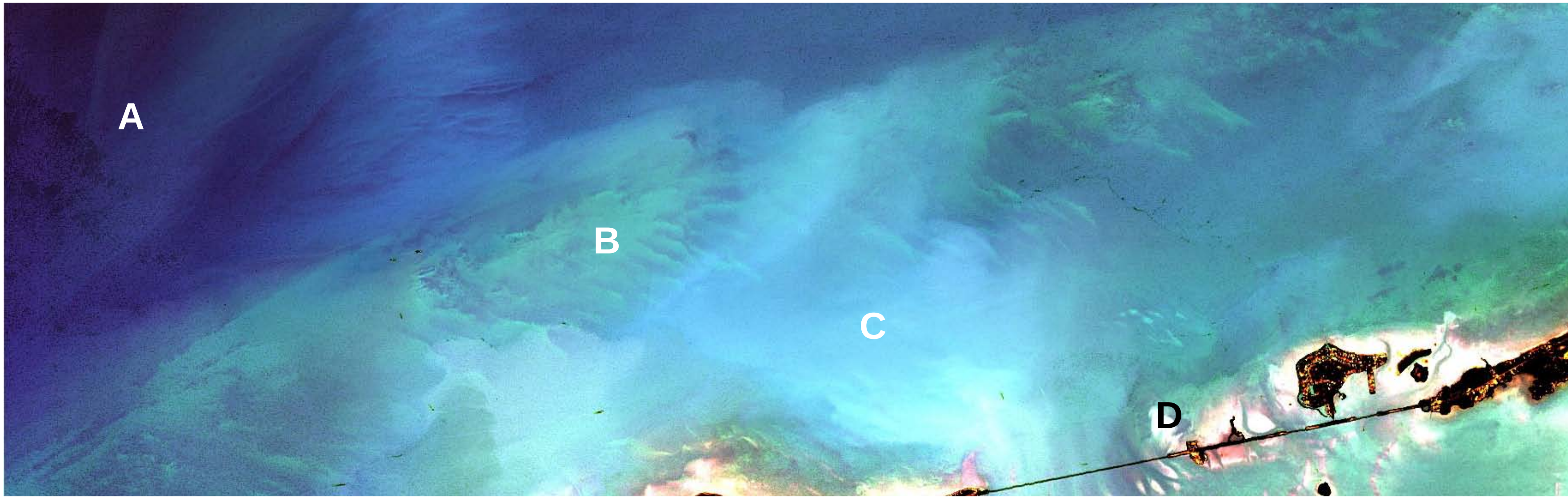

AVIRIS data were atmospherically corrected for ocean scenes. The data are corrected for skylight reflected off the sea surface. It is assumed that the water leaving radiance is 0 for wavelengths greater than 1.0 micron. Note how all of the spectra are 0 past 0.82 micron. (B.-C. Gao, M. J. Montes, Z. Ahmad, and C. O. Davis, *Appl. Opt.* 39, 887-896, 2000.)

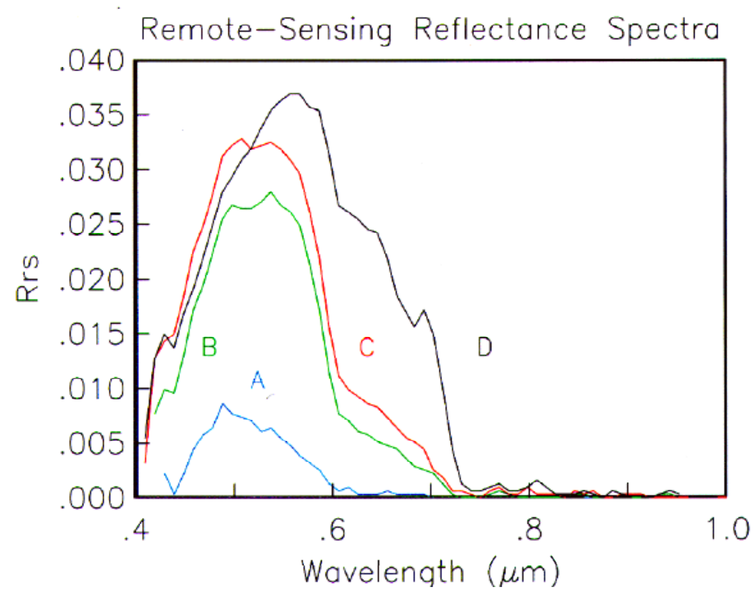

Sunglint Effect Removal With An Empirical Technique

Sunglint effect becomes stronger from left to right in an AVIRIS image. Individual wave facets are observed in the high spatial resolution AVIRIS image (20 m). It is not possible to use Cox & Munk model to predict sun glint effects in this case.

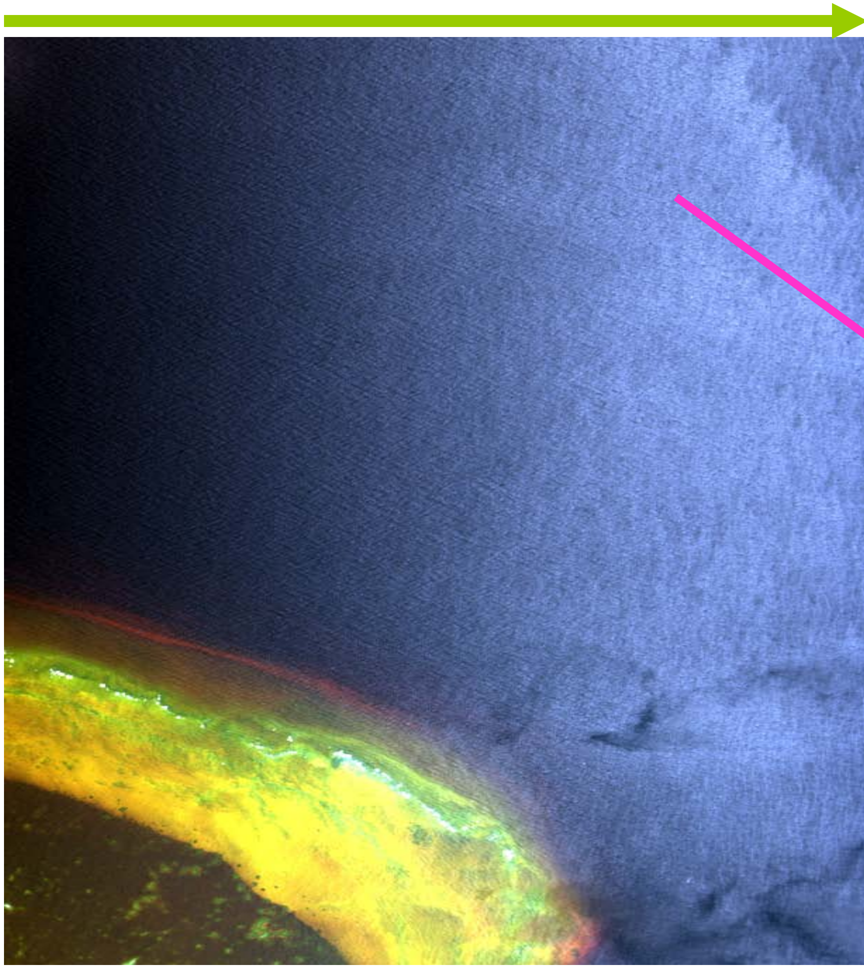

A sample sunglint apparent reflectance spectrum

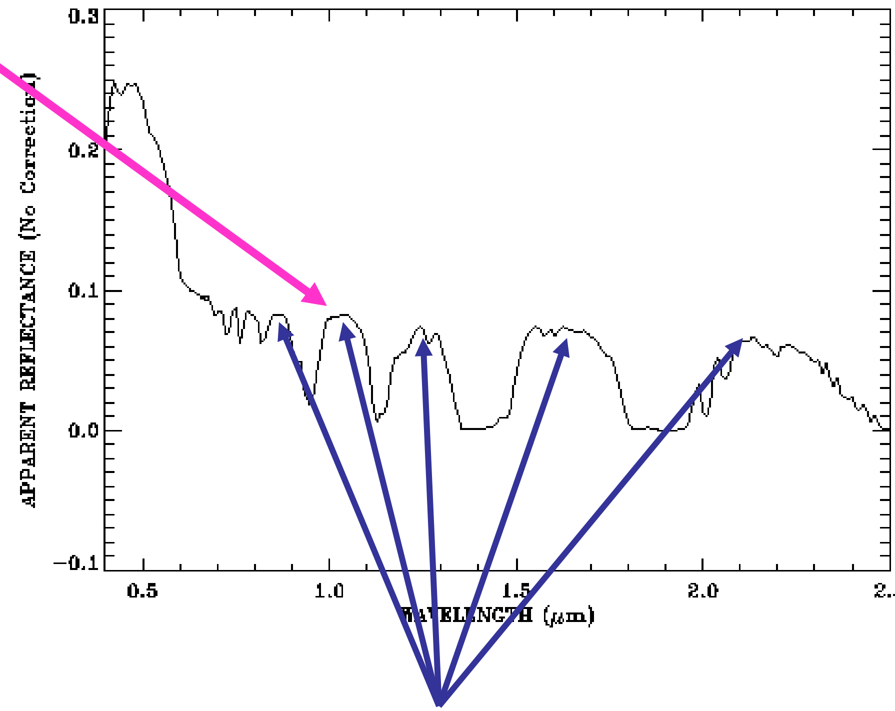

The sunglint reflectances for atmospheric window channels above 0.8 micron are almost constant. The empirical technique = ATREM (Land) reflectance minus 1.04 micron reflectance value on the pixel by pixel basis.

Images Before and After The Empirical Sunglint Correction

Before

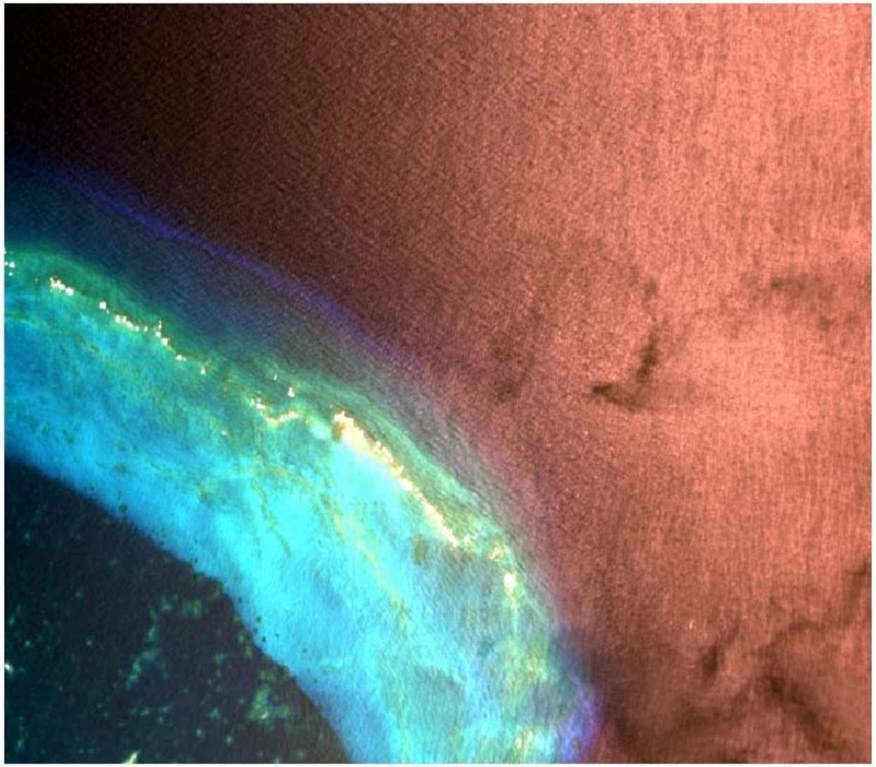

After

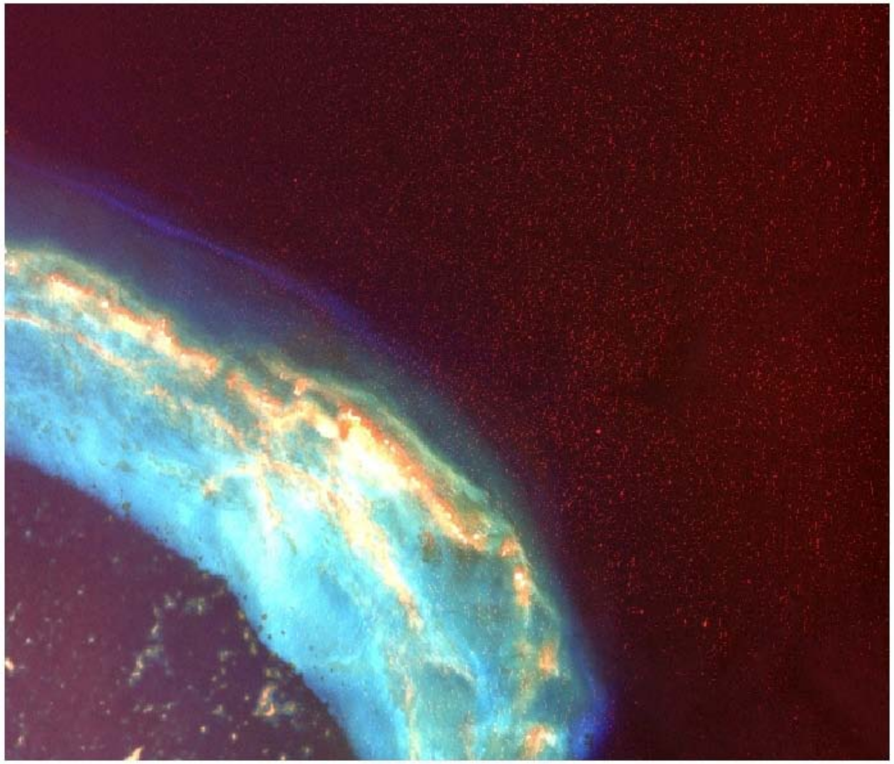

The image at right demonstrates that, after the empirical correction, the sunglint effects are mostly removed. The “contiguous” spatial features in the middle bottom portions of the image are seen much better. However, minor noise effects are seen in areas without bottom reflection.

Second Case of Glint Removal Using AVIRIS Data Over Kaneohe Bay, HI

Before

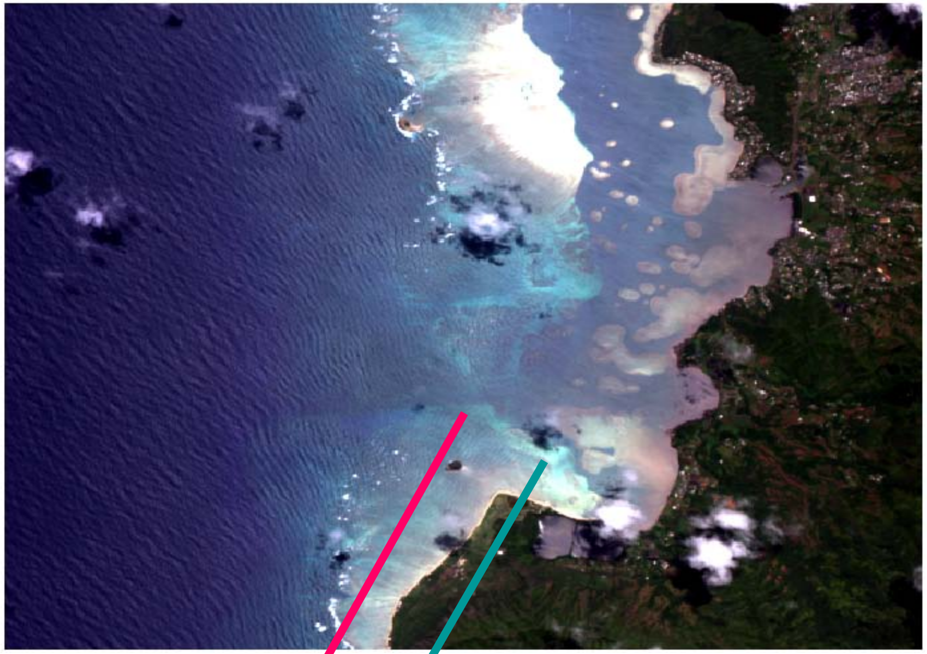

After

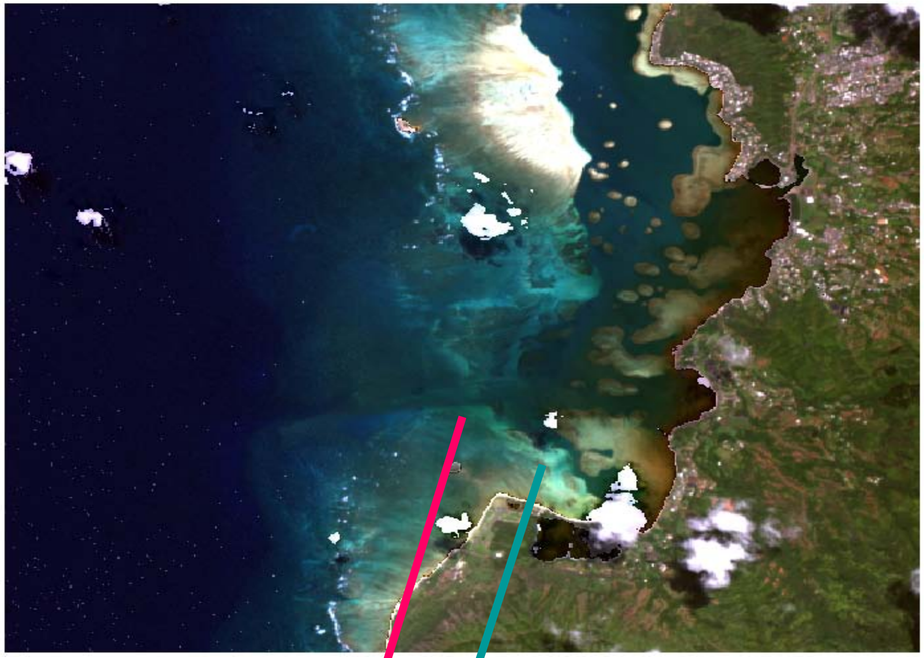

Sample Radiance Spectra

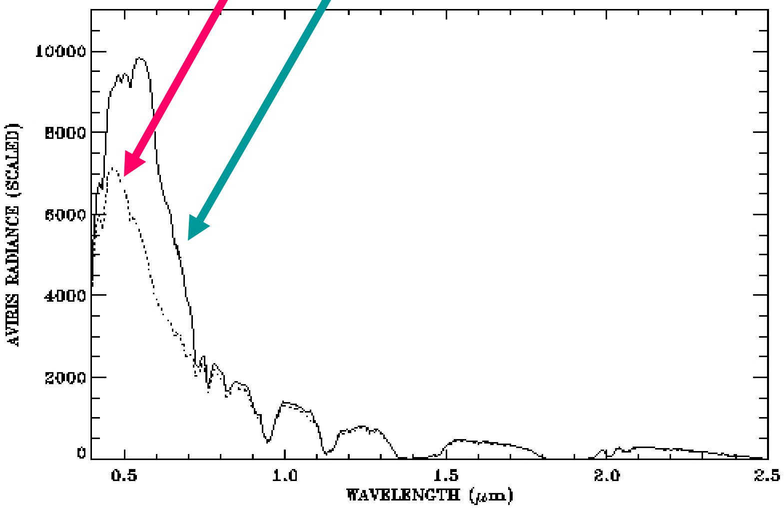

Sample Derived Reflectance Spectra

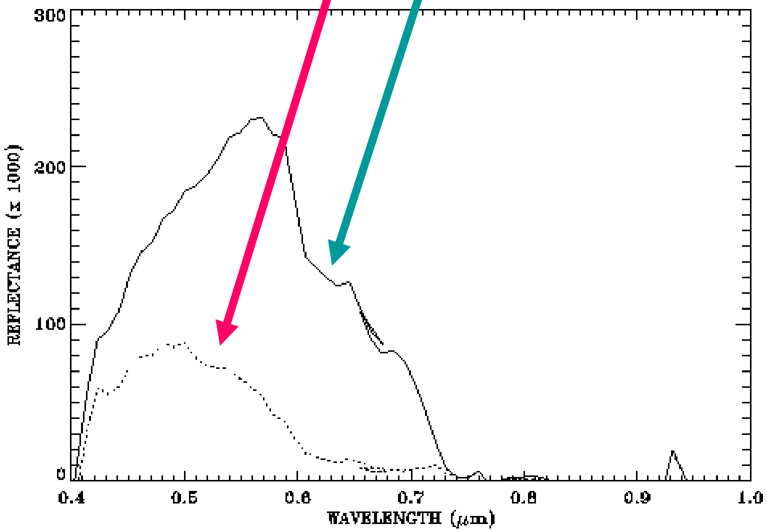

Earth Surface Images from HICO

Images are about 43 km wide and 190 km long

Orientations are given below

Cape Town, South Africa, Oct. 3, 2009. Orientation is from NW at top to SE at bottom.

Lower Chesapeake Bay, Oct. 7, 2009. Orientation is from NW at top to SE at bottom.

Coast of South China Sea, near Hong Kong, China, Oct. 2, 2009. Orientation is from SW at bottom to NE at top.

Part of the Grand Canyon, Sept. 27, 2009. The center of the image is at 35° 50' N, 111° 23' W and the orientation is from SW at bottom to NE at top.

Florida Keys, over Key Largo, Sept. 27, 2009. Orientation is from SW at bottom to NE at top.

Sahara Desert over Egypt, Sept. 27, 2009. Orientation is from SW at bottom to NE at top.

Taken over the Bahamas, Oct. 2, 2009. Orientation is from NW at top to SE at bottom.

Gem of the Pacific. Midway Island, Sept. 27, 2009. Orientation is from NW at top to SE at bottom.

HICO RGB Image & Sample Spectra of Florida Keys

Examples of an ASD Spectrum and a Water Leaving Reflectance Spectrum Retrieved From HICO Data Over Florida Keys

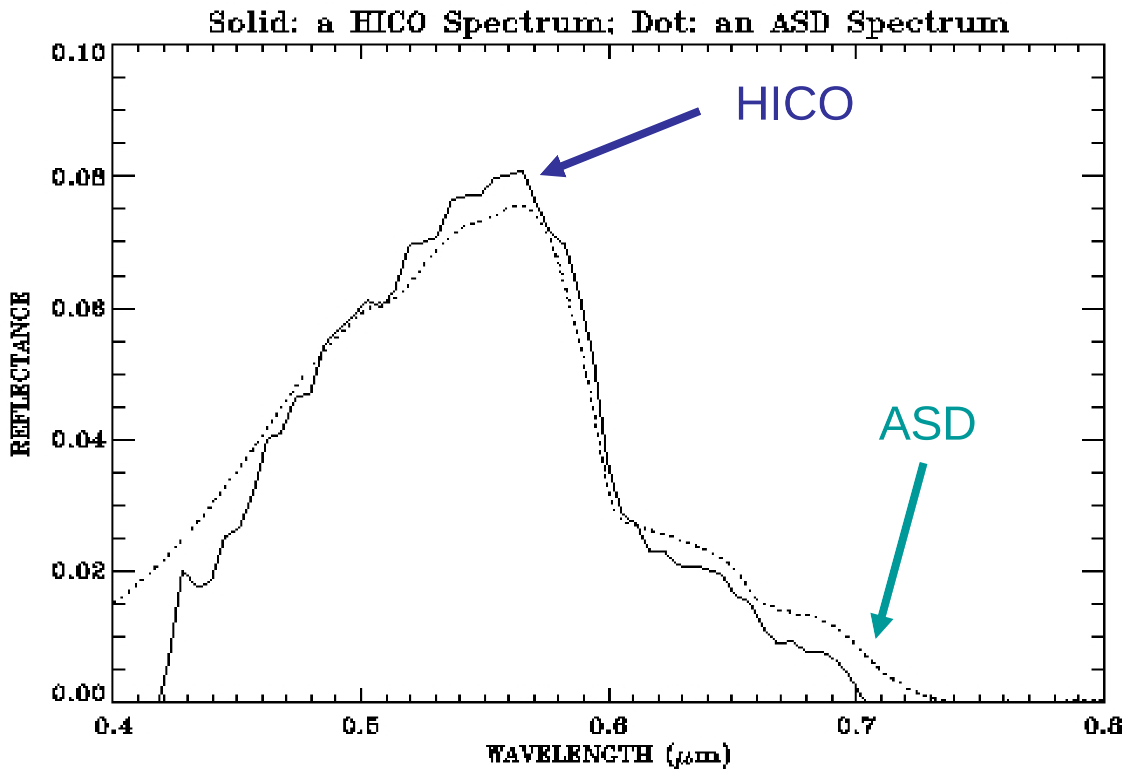

Please note that the shapes of the two spectra in the 0.45 – 0.8 micron wavelength Interval are very similar. The two spectra are not measured over the same time, nor over the same spatial location.

Summary

- At present, both the land and ocean version of the algorithms work well under typical atmospheric conditions.

- In the presence of absorbing aerosols, the model tends to overestimate the atmospheric contribution to the upwelling radiance, resulting in inferred surface reflectances which are biased low in the blue region of the spectrum.

- Upgrades to the atmospheric correction algorithms are planned, particularly in view of major advances in aerosol models. Specific upgrades include:
    - Incorporation of absorbing aerosol models
    - Incorporation of UV channels (380 nm, 400 nm)

- An algorithm theoretical basis document for HyspIRI Level 2 at surface reflectance (land) and remote sensing reflectance (shallow water) is under development.